

## Investigation of the value and mechanism of atmospheric plasmoid charge formation

© S.I. Stepanov

St. Petersburg Nuclear Physics Institute, National Research Center Kurchatov Institute, Gatchina, Russia  
e-mail: stepanovsmail@googlemail.com

Received July 6, 2022

Revised October 27, 2022

Accepted October 31, 2022

The study of a long-lived atmospheric plasmoid has been continued. (Gatchina plasmoid). The electric charge of the plasmoid was detected earlier by us using a plasma probe. Here the measuring equipment was improved, which allowed to take into account the influence of bias current. The measured charge of the negative plasmoid was about  $-35$  nC. The cause of the electric charge is investigated. It consists in the inhomogeneity of the plasma and, as a consequence, a special configuration of the electric field during discharge. In the column of emission plasma above the central electrode, the field is directed into the plasmoid (for positive central electrode). In streamers coming out of the plasmoid and in space above the plasmoid, the field is directed outward. To find out the reason for the appearance of the charge, the Gauss theorem is applied. The column of emission plasma gives a small contribution to the integral. The integral will be determined by the second section having a different sign. Thus, the plasmoid has a charge during discharge. After the current is turned off, the charge is retained due to the rapid cooling of the plasma. It is noted that when obtaining other long-lived plasmoids, there is a similar configuration of the field during discharge. A similar discharge structure occurs when a linear lightning strikes the electric network and a ball lightning appears from an electrical outlet, a speaker, etc. This work introduces a new object of plasma physics a charged atmospheric plasmoid.

**Keywords:** atmospheric plasmoid, high-voltage discharge, plasma probe, ball lightning, electric charge.

DOI: 10.21883/TP.2023.01.55440.179-22

### Introduction

The long-lived atmospheric plasmoids existing after turning off the discharge current have been obtained many times [1–4]. When obtaining the plasmoids, the electrodes erode, thereby determining a composition and properties of the plasma.

In 2001, in the atmospheric conditions a long-lived plasmoid (Gatchina plasmoid) was obtained, which was well reproduced, for example, in [5–8]. The plasmoid (Fig. 1) occurs in the high-voltage discharge between the graphite or metal electrode 2 and the water surface, in which another electrode is inserted 3. The discharge current lasts for 100–150 ms, then the plasmoid exists autonomously. The time of visible observation is up to 500–600 ms, so is that of infrared observation — up to 1200 ms [9]. The structure, motion and temperature are successfully investigated not only experimentally, but using a method of numerical gas dynamic simulation [10,11].

Since 1960s and up to now, there is a hypothesis of energy storage in the long-lived luminous plasma bodies remaining after irradiation of air with radiowaves [12] and in the Gatchina plasmoid [13]. The hypothesis says that the energy is stored in meta-stable states of oxygen molecules.

There are electric discharges, like sparks, arcs, etc., which are observed between the ball lightning (BL) and conducting, in particular, grounded items [14]. It is usually

explained by the fact that the ball lightning has an electric charge [15,16]. These phenomena are described in the popular magazine „Technics — to youth“ dated 1982 (the number 3, p. 38): „When a glaring ball approached me for about five meters, my hair had started rising. I felt that even small hair on the hand and the chest were tensioned toward the lightning as it was usually the case when adjusting the high-voltage equipment. Moreover, the „small threads“ were stretched from the chest towards the ball lightning. Fortunately, the ball had just passed me in 3–4 meters“.

A charge of the ball lightning is always present in the hypotheses of the ball lightning motion at the constant elevation above the ground [11,16,17].

The similarity of some properties of the plasmoid and the ball lightning has compelled us to check presence of the electrical charge in the plasmoid. The plasmoid charge was discovered in 2008 [18]. The plasmoid charge was measured by using the Langmuir probe as well as a modified probe manufactured as the metal grid. The probe measurements showed the charge  $-12.5$  nC within the time period 170–220 ms since turning on the discharge current; while the grid measurements have provided  $-15$  nC within the time period 300–470 ms. The probe signal starts with a current peak. In another experiment scheme the Langmuir probe was used for measuring the potential difference between the central electrode and the plasmoid [19].

The present work is aimed at improving the charge measurement method and measuring the charge in dependence on the polarity of the electrodes and the lifetime of the plasmoid. Theoretically, the present work is aimed at clarifying the mechanism of origination of the electric charge.

## 1. Unit for obtaining and investigating the plasmoid

The plasmoid was obtained by using the unit (Fig. 1), which was previously used [20] and it is a modification of the original unit [6–8]. The discharger is the vessel with water 1, which comprises two electrodes. The central graphite electrode 2 extends above the water surface by 2–3 mm. It is isolated from water by a quartz tube. Prior to turning on the charge, the central electrode is wetted with some water, 10–20  $\mu\text{l}$ . The ring electrode 3 is on the vessel bottom. The wires powering the electrodes pass

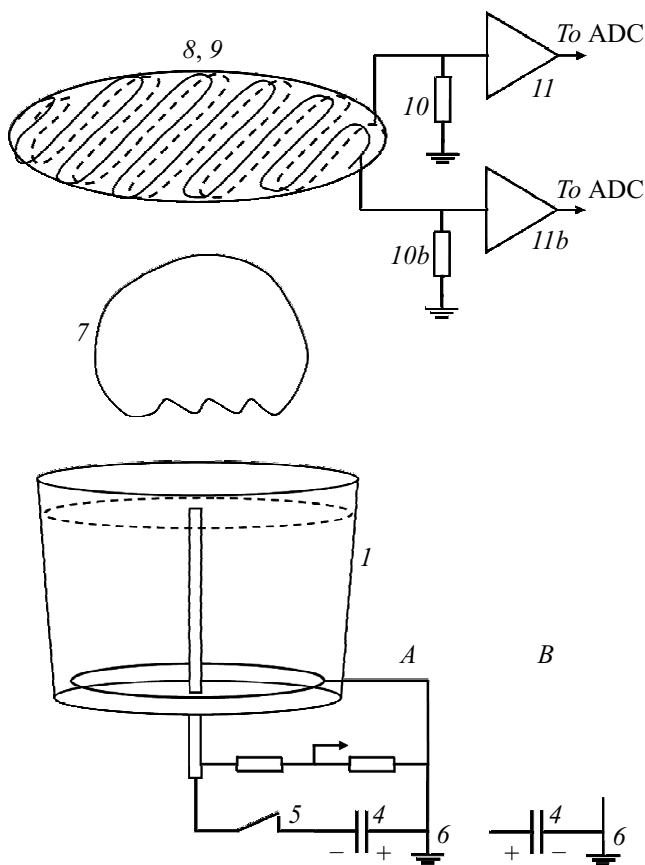


**Figure 1.** Device for obtaining the plasmoid and measuring its electric charge: 1 — the vessel with water, 2 — the central electrode, 3 — the ring electrode, 4 — the high-voltage condenser, 5 — the high-voltage switch, 6 — the grounding (the common wire), 7 — the plasmoid, 8 — the grid made of uninsulated wire (bare grid), 9 — the insulated grid, 10 — the resistors, 11 — the amplifiers. The electric connections used in the present work: A — the water is an anode; B — the water is a cathode. The ring electrode is always grounded.

through the vessel bottom. It provides a symmetrical electric field above the vessel during the discharge. It is assumed that the plasmoid is formed as more symmetric and less deviates from the vertical. The vessel was filled with faucet water with one third of distilled water. The previous tests have determined that this water composition ensures good reproduction of the plasmoid [5–7]. The discharge was obtained by applying the voltage 5 kV from the condenser bank 4 of the capacitance 700  $\mu\text{F}$  to the electrodes. The discharge lasted for 130 ms. The discharge was turned on/off using a high-voltage switch 5, which was manufactured in the laboratory and previously used for obtaining the plasmoid [20]. The switch was designed [21] so as to provide quick turn-off of the discharge. When turning off, the arc is pulled by a magnetic field into a slit between the dielectric plates to be quickly cooled therein. Thus, there is no potential on the central electrode, hence, no electric field from the electrodes above the vessel in the autonomous phase of plasmoid existence.

There are two possible circuits for connecting the electrodes to the high-voltage source, which differ in the discharge current direction (Fig. 1). Type A: the central electrode — is the cathode, the water — is the anode. Type B: the water — is the cathode, the central electrode — is the anode. The electrode processes in these discharges differ, so it should not be expected that the properties of these two plasmoids (hereinafter referred to as the plasmoids of the type A and B, respectively) will completely coincide. The polarity of the type A was used in the works [5–9, 18–20, 22–34], while the works [35–38] have used the polarity of the type B.

The measurement instrument (the Langmuir probe or the grid) measures the voltage and the current in relation to the reference (grounded) electrode, whose potential is assumed to be zero. Thus, when investigating the plasmoid of a certain type, for example, the type A, the results will depend on the electrode being selected a reference one. For the reference electrode, this investigation has selected the ring electrode immersed in water. The reference electrode is grounded, i.e. it is connected to the grounded wires of the analogue-digital converter, the computer and the power mains of the laboratory. The grids are connected to the reference electrode via resistors (10, Fig. 1).

The tests have recorded the voltage of the central electrode, the discharge current, the plasmoid luminosity, the net signals. The measurement interval was 1 ms. Simultaneously, the video recording was carried out with the interval 33 ms between the frames. A mirror was installed above the vessel with water, thereby making the plasmoid visible in a side view and in a top view on each frame. It made it possible to better view the shape of the plasmoid and its deviation from the vertical axis of symmetry. The plasmoids of the types A and B were shot using the same camera. The shooting is exemplified below (see Section 5, Fig. 4). As it is clear from this example, the glow of the plasmoid is first spherical to become ring-like later. The ring is observed to 300–500 ms in visible light, for

example, in the work [9], and to 1500 ms in the infrared light (ibidem). The authors of the work [39] publish a photo made during their investigations. The photo shows arrows which indicate an expected motion of the plasma during plasmoid formation (ibidem, Fig. 7). The plasma jet generates the plasma upwards into the plasmoid. At this moment, the plasmoid is a ring-like plasma vortex having a toroidal rotation (ibidem). This scheme is matched with results of the gas dynamic mathematic simulation, which is mentioned above [10,11].

Judging by the video records, the plasmoids of the types *A* and *B* have turned out to be not exactly the same. The average measured lifetime of the plasmoid of the type *A* was 550 ms, so was that of the type *B* — 390 ms. The maximum time — 625 and 410 ms, respectively. The radii of the plasmoids *A* have turned out to be in average by 20% bigger than the radii of the plasmoids of the type *B*, hence their volumes differ by 70%.

## 2. Principle and device for measuring the plasmoid charge

The charge measurement principle is based on the fact that the plasmoid charge creates the electric field between the plasmoid and the grounded grid. The grid collects the charged particles of the plasmoid which come to it. The particles move due to drift in the electric field and diffusion. The grid signal is fed to the amplifier and then to the measurement device. Several conditions are necessary for the charge measurement. The data on the plasmoid charge are provided by a part of the grid current, which is a drift current. Let, for example, the plasmoid have a negative charge. Then the plasmoid potential is negative in relation to the grounded grid. The negative particles (electrons, negative ions) drift into the plasmoid field towards the grid and transmit their charge to it. As the plasmoid passes through the grid, its charge decreases and at the same time the electric field and the drift current decrease. It results in incomplete accumulation of the charges.

It is obvious that the unit should be assembled so as to create the electric field near the grid only by the plasmoid charge. Then, provided that the drift current is bigger than other currents, in particular, bigger than the diffusion current, the charge is equal to the grid current integrated for the time of the plasmoid passing through the grid.

The drift and diffusion currents of the charged particles of any kind are determined, in particular, by the concentration of these particles. The measurements show that the concentration of the charged particles in the plasmoid decreases in time. The concentration of the electrons in the plasmoid was evaluated by the Stark effect to have the values  $(300, 8, 0.3, 0.08, 0.02, 0.01) \cdot 10^{20} \text{ m}^{-3}$  at the time (3, 70, 95, 115, 175, 225) ms, respectively [19]. The CaII ion is detected in the plasmoid at earlier periods of time on the resonance lines 393.4 and 396.7 nm [19,26]. The decrease of the concentration of this ion may be evaluated

by the change of the line intensity, which was (70, 2, 0.15) conventional units at the time (15, 75, 135) ms [19].

The measurements using the thermocouple [19,24] and by the speed of ultrasound passing through the plasmoid [20] show that as the plasmoid exists its temperature decreases. The temperature decrease contributes to recombination of the charged particles. The presence of water vapor results in formation of cluster ions with water molecules; they were observed using the mass-spectrometry [33]. The tests [34] have observed a smoke ring rising at the end of plasmoid glow and after extinguishing of the glow. Due to the recombination and the increase of the masses of the charged particles, the drift current decreases, so when the plasmoid flies through the grid, there is incomplete accumulation of the charges. This effect is the greater, when the lifetime of the plasmoid is greater. In order to reduce this effect, the grid shall be designed with a minimum mesh size. However, this grid perturbs the plasmoid motion. The same aim should also be sought by carrying out the measurements when the mobility of the charged particles is still big, i.e. soon after formation of the plasmoid. For this, the grid should be arranged at the minimum height. However, this option can exhibit a high-current discharge between the central electrode and the grid with damage of the equipment.

Naturally, the grid is also sensitive to the bias current caused by variation of the electric field in time near the grid. This current occurs because the charged plasmoid approached the grid and also because the plasmoid charge decreases during the measurement itself. These effects act oppositely. It has been found in the preliminary tests that the bias current was comparable in value to the current of the charged particles. Hence, the bias current introduces an error to the charge measurement. In order to take into account this current, these tests have used an additional grid (9, Fig. 1). The grid is made of an insulated wire, thereby excluding the flow of the charged particles to it. Therefore, the insulated grid can measure the bias current only. Both the grids are located in one plane in order to ensure the same sensitivity thereof to the bias current. Subtracting the signal of the insulated grid from the signal of the bare grid, we obtain the signal due to the charges collected by the bare grid. By integrating this signal, we obtain the plasmoid charge.

The grids are connected to the identical resistors *I0* and *I0b* (5 M $\Omega$ ); and the amplifiers *I1* and *I1b* were also identical. The bare grid is made of a nickel-chromium wire of the diameter of 0.2 mm. The insulated grid was made of the copper wire of the diameter of 0.5 mm with fluoroplastic insulation of the thickness of 0.25 mm. The double grid had the diameter of 20 cm. The double grid was adjusted by placing a plate nearby and energizing it with alternating voltage. If subtracting the signals provides zero, then the bias currents of both the nets are the same and the device is correctly operated. Hereinafter, this grid will be referred to as „the grid“ or „the sensor“. In order to reduce the influence of the external fields, a grounded metal framed

was placed around the grid, it was sized as  $0.6 \times 0.6$  m and it is not shown on Fig. 1.

### 3. Obtaining the charge value from the measurement data

The signals occurring during the double net's measurement are shown on Fig. 2 for the negative plasmoid. Both the grids exhibit the currents *I* and *3* during the discharge. These are bias currents originating from the electric field of the rising plasmoid. This is the first result of this investigation: the rising plasmoid really carries the charge, whose field creates the bias current. As the sensitivity of both the grids to the alternating field was the same, the currents *I* and *3* have turned out to be the same.

During the plasmoid flight through a grid plane (this moment was determined by the video records), a current is produced in the circuit of the insulated grid *4*. It is the bias current. The bias currents *3* and *4* in the circuit of the insulated grid have opposite directions. In fact, the first one is caused by the increase of the field (in absolute magnitude) during the discharge, so is the second one by the decrease of this field for the time of the plasmoid transit through the grid. As noted above, this occurs due to drain of the plasmoid charge to the bare grid.

During the plasmoid flight, the current *2* is recorded in the circuit of the bare grid. As noted, it is a sum of the current of the charged particles and the bias current.

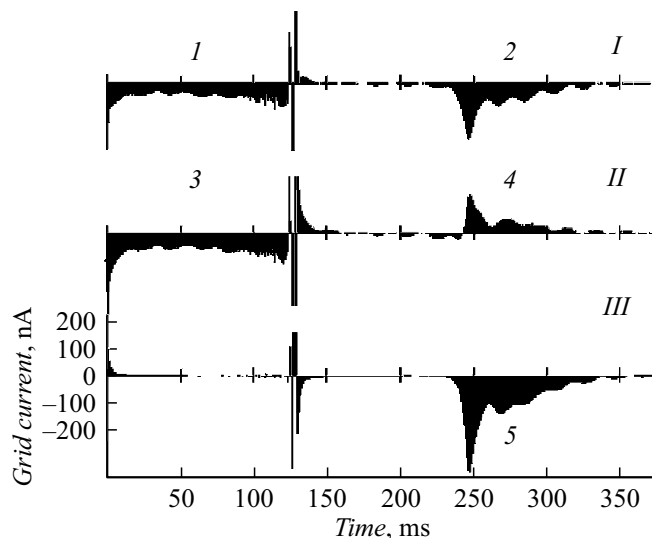


**Figure 2.** Currents of the grids of the negative plasmoid. Test №. 5022. *I* — the current of the bare net. It consists of the bias current during the discharge (*1*) and the current originating during the plasmoid flight through the grid (*2*). *II* — the current of the insulated grid. It consists of the bias current during the discharge (*3*) and the bias current in the plasmoid flight through the grid (*4*). *III* — the difference of the currents of the bare and insulated grids. This plot consists of the current of the charged particles to the bare grid only (*5*).

The data was processed by subtracting the current of the insulated grid *II* from the current of the bare grid *I*. As a result, the plot *III* has been obtained. It has only the current *5* now. It is a current originating in collision of the charged particles with the bare grid. As said above, it is the sum of the drift and diffusion current. This test exhibits the negative current, so the plasmoid current is negative. It agrees with the fact that in this test the potential of the central electrode was negative (the scheme *A*, Fig. 1). At the moments of turning on/off the discharge current, the difference plot *III* still has short signals as well.

The whole length of the plots of the grid currents *I* and *II* has visible oscillations of the frequency of 50 Hz. Probably, these are the bias currents caused by the alternating external field created by the electric wiring and the instruments in the laboratory. Naturally, this difference plot is without these oscillations. However, this plot also has the oscillations of the signal of the same frequency at the time of the plasmoid transfer through the sensor, i.e. within the time interval 230–350 ms. Probably, these oscillations have another cause, which is not the bias current, but it is the periodic change of the drift current to the bare grid under impact of this external electric field. Thus, the external field causes two effects, i.e. the bias currents and the modulation of the current of the particles to the bare grid. The plots are analyzed to show that the phases of the two oscillations differ by  $90^\circ$  as follows from the nature of the currents.

The charge currents *5* of Fig. 2 are characterized by a big peak at first, which originates when the plasmoid touches the grid. This peak was always when the grid was at the small height, and in a part of the tests when the grid was placed at the average height. This current peak may be related to a sharp upper border of the plasmoid as detected by the various methods. The works [18,19,23] have investigated the plasmoid of the type *A* using the single Langmuir probe. The probe signal also starts from the sharp current peak [18]. The sharp boundary at the plasmoid top is detected at the video records [20,23,24] on the schlieren photos [27]. The tests have been carried out to divert the laser beam by the rising plasmoid [25]. The author of the works [25] explains the test results by sharp decrease of the temperature and jump of concentration of the molecules at the upper border of the plasmoid.

### 4. Charges of the positive and negative plasmoids

The charges of the plasmoids of the types *A* and *B* are measured by the sensor from the two double grids located one above the other. The signals from the grids were summed. The second grid was used for improvement of accumulation of the charges. The sensor is surrounded by a shielding grounded ring. The sensor was installed by 20–38 cm higher than the central electrode. Thus, the charge was measured at the various time of plasmoid existence. The measurement data are shown in Fig. 3.

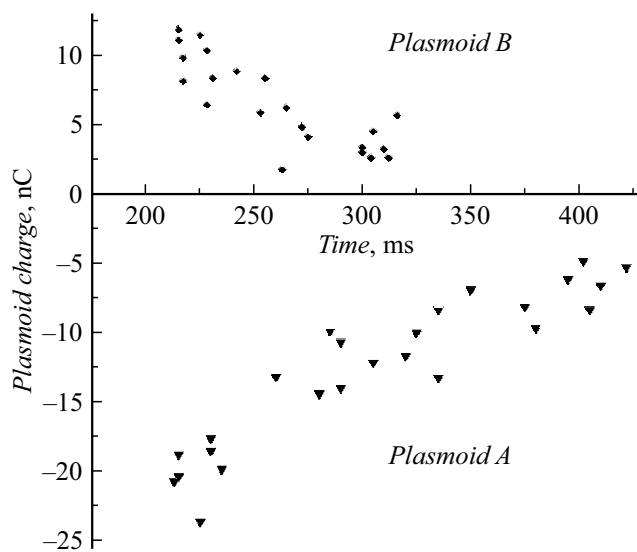


**Figure 3.** Charges of the plasmoids of the type A (the central electrode is negative) and the plasmoids of the type B (the central electrode is positive) depending on the time between the charge beginning and the maximum current of Fig. 2,(5). The discharged was terminated at the time 130 ms. The tests were carried out using the sensor consisting of the two double grids of the diameter of 20 cm, which are located one above the other. The grids are surrounded by the shielding ring.

As expected, the charge of the plasmoid of the type A is negative, and that of the type B is positive. The charge is a remaining magnitude, but the measured charges decrease in time. It is caused by the fact that the mobility and the concentration of the charged particles decrease in time and, as a consequence, the drift current decreases. Another possible cause is that the diameter of the plasmoid and its deviation from the vertical increase in time, so that the part of the plasmoid passes past the grid.

It is clear from Fig. 3 that the measured charges of the negative plasmoids A are almost in more than two times bigger (in absolute magnitude) than the charges of the positive plasmoids B. Let us specify possible causes thereof.

1) At the moment of current break the condenser still has voltage (various in absolute magnitude). However, the measurements have shown that the voltage was the same (2.5 kV), so this version should be declined.

2) The drift current is caused by different particles. In the negative discharge of the type A the current is created by drift of electrons and negative ions to the grid. In the positive discharge the drift current is created by motion of the positive ions only. Due to much bigger mobility of the electrons the drift current in the plasmoid of the type A can be bigger than in the plasmoid B, *ceteris paribus*.

3) The difference of the charges of the positive and negative plasmoids can be related to the difference of their sizes. This version will be discussed below.

Using the results of Fig. 3, it can be evaluated which charge was at the plasmoid at the end of the discharge

current (130 ms). For this the curves of Fig. 3 were extrapolated. The extrapolation shows that at this moment the charge of the negative plasmoid was about  $-35$  nC.

Let us evaluate the volume (excessive) concentration of the charges creating this charge. It is equal to (the plasmoid charge/the electron charge)/the plasmoid volume. It is  $0.62 \cdot 10^{14} \text{ m}^{-3}$ . Thus, at the time 225 ms [19] the excessive concentration is in 16000 times less than the evaluated full concentration of electrons  $0.01 \cdot 10^{20} \text{ m}^{-3}$ , which is mentioned in Section 2.

## 5. On distribution of the electric charge in the plasmoid

This interesting question was studied by comparing the plots of the current of the charged particles (the current 5, Fig. 2) and via the simultaneous video recording of the same plasmoids. The negative plasmoid is exemplified on Fig. 4.

### 5.1. The first observation

Let us compare the first two frames taken at the time 256 and 290 ms. At the both frames, the plasmoid has not arrived to the grid. At the time 256 ms there is no current, but at the later time 290 ms there is the current, although the plasmoid is still below the grid by 2–3 cm, i.e. the current of the charged particles to the grid appeared before arrival of the luminous top of the plasmoid to the grid. This relationship was obvious in all the tests. Probably, the electric charge is above the glow area.

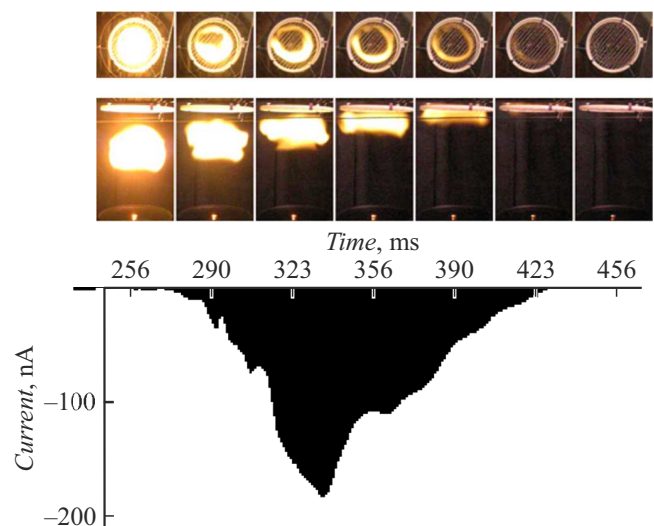


**Figure 4.** Plot of the current of the charged particles (the current 5, Fig. 2) of the negative plasmoid (the test №. 4808) and the frames of the simultaneous video recording of the same plasmoid, which are taken at the time 256–456 ms from the start of the discharge current. A lower part of each frame is a side view, while the upper part is a top view obtained by a mirror.

## 5.2. The second observation

Let us compare the frames taken at the time 390, 423, 456 ms. The frame 390 ms has both the current and the glowing plasmoid which is directly under the grid. At the same time, there is no glow above the grid. The frame 423 ms has a very little current and low glowing. The frame 456 ms has neither current nor glowing, i.e. the current terminates with termination of the glow. This relationship is clear in the tests, when the grid is located at the middle and top height. If the grid was at the small height, then after termination of the current the weak glow of the plasmoid was still observed above the grid.

## 6. On mechanism of formation of the electric charge in the plasmoid

Let us consider this question based on the video records of the plasmoid and the measurements of its electric properties. The detailed photos of the plasmoid and the explanations thereto have been published before [30,32]. Fig. 7,*j* of the work [32] is a base for Fig. 5 of the present work. The frame was taken in the middle of the current stage, 60 ms.

Just after turning on the current, there is a brightly luminous jet 3 appearing above the central electrode 2. In the English literature, it is referred to as „plasma channel“ [28] and „jet“, whereas the latter is applied more often [9,26,29,31,35]. In the Russian literature, it is referred to as „struya“ [32]. The jet is slightly changing in time. At this moment the lower part of the jet is expanded, while the upper part is thin.

The plasmoid 5 is on top of the jet. The blue streamers 4 start at a lower part of the plasmoid and terminate on water. In the literature, they are referred to as „a spider, spider-like structure“ as they have a characteristic appearance [31]. As

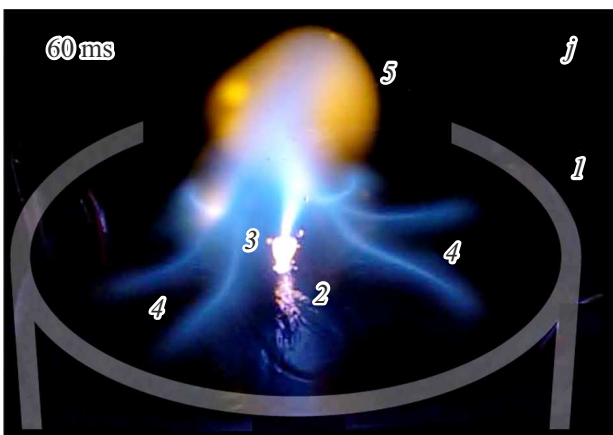


**Figure 5.** Structure of the discharge creating the plasmoid. The picture is drawn as per Fig. 7,*j* of the work [33]. 1 — the vessel with water, 2 — the central electrode (its image is distorted by the water waves), 3 — the plasma jet above the central electrode, 4 — the streamers, 5 — the plasmoid.

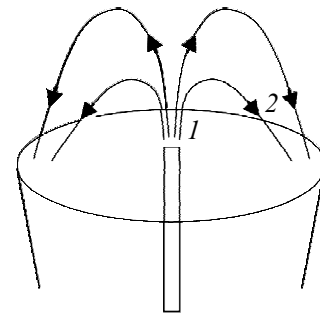


**Figure 6.** The current path during the discharge. 1 — the plasma jet, 2 — the streamers. Like Fig. 7, this figure is drawn for the positive plasmoid.

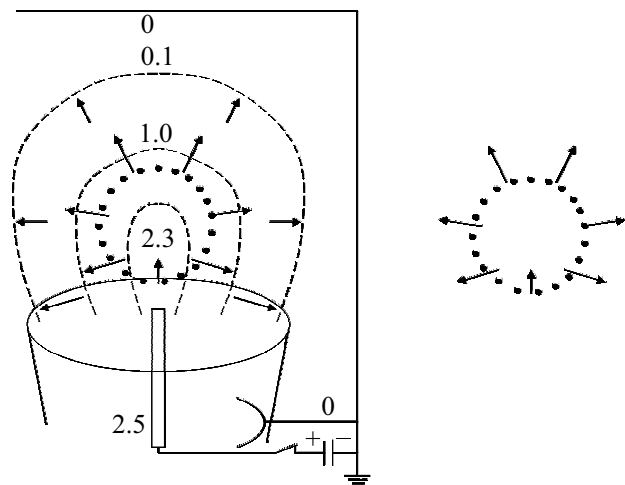


**Figure 7.** Approximate distribution of the potential (in kilovolts) and the electric field (the arrows) during the discharge. The potential values 2.5 and 0.0 are exact, while 2.3 is obtained in the measurements, the values 1.0 and 0.1 are extrapolated ones. The top shows in a simplified form the grounded frame, it is located at the height of 1 m above the jar. The dots outline the surface which is used for application of the Gauss theorem. This surface with electric fields thereon is shown at the right side separately.

the height of the plasma jet increases, the streamers and the plasmoid are also lifted. The work [30] states that the blue color of the streamers is caused by calcium radiation (the Ca I line at 420 nm). The radiation of the plasma jet is determined, in particular, by H-alpha and OH radicals, whereas the yellow color at the cold border of the plasmoid originates from the sodium lines (ibidem).

As it is clear from the earlier works, the discharge current flows along the plasma jet and then through the plasmoid and the streamers to water. The current path is shown on Fig. 6. The plasma glows in the jet much more intensely than in the streamers. Figures 6 and 7 are drawn for the positive plasmoid.

At the end of the current phase the streamers merge into a solid skirt. After turning off the discharge, the plasma in the

skirt glows for some time, while the plasma jet immediately distinguishes.

Let us compare the current densities in the jet and the streamers. The current cross-section in the jet (let its radius be equal to the electrode radius, i.e. 3 mm) is approximately  $\pi \cdot 3^2 \approx 28 \text{ mm}^2$ , while the section of the same current in the skirt above the water surface (the vessel radius is 100 mm) is  $\pi \cdot 100^2 = 31\,400 \text{ mm}^2$ . The area ratio is 1100. Thus, the density of the current entering the plasmoid through the plasma jet is significantly higher than the density of the same current exiting the plasmoid through the streamers. From comparison of the current density and the intensity of the plasma glowing in the jet and the streamers, it is clear that the volume power output in the jet is significantly bigger than in the streamers.

In the records given in the various works, as well as taken in the present work, it is clear that before turning off the charge (the time period 110–130 ms) the skirt plasma glows near the central electrode, while it has no glow at the vessel periphery. It well agrees with the low current density of the periphery area.

The approximate distribution of the potential in the second half of the discharge is shown on Fig. 7. The following data are used for the figure. The potential of the surrounding equipment (the frame, the measurement grid, the ring electrode) is zero. Before turning off the current, the central electrode has the potential +2.5 kV. These data are known for sure and shown on the figure. As mentioned above, the works [19,24] have measured the difference of the potentials between the central electrode and the plasmoid at the height 20 cm. At the end of the current phase this value was 0.2 kV. Based on these measurements, the potential of the plasmoid of Fig. 7 is indicated as  $2.3 \text{ kV} = 2.5 - 0.2 \text{ kV}$ . These data were sufficient to construct the approximate distribution of the potential within the intermediate area. It has turned out that the main part of the applied voltage drops at the streamers between the plasmoid and water.

From the data on the potential and the current it is easy to restore the distribution of the electric field at the end of the current phase. It is shown on Fig. 7. The field in the plasma jet above the central electrode is directed inward the plasmoid. Thanks to the high power output, the conductivity of the plasma in the jet is high, while the field is small. It also follows from the probe measurements. At the same time, in the streamers and above the plasmoid the field is directed outward the plasmoid and it is higher than in the plasma jet. In the final picture, the field distribution everywhere agrees with the distribution of the potential in accordance with the formula  $E = -\text{grad}\varphi$ , as expected. In addition, the field direction everywhere agrees with the current direction, as it should be.

We are summing. The current entering the plasmoid flows through the plasma jet above the central electrode. Here, the electric conductivity is high, and the electric field is low. The field is directed inward the plasmoid. The current exiting the plasmoid flows within an area of the high electric field in the streamers. The field is directed outward the plasmoid.

In accordance with the Gauss theorem, the electric charge within a certain volume is proportional to the integral  $\int E_n ds$  across the closed surface around the volume, where  $E_n$  — a normal component of the field,  $ds$  — a surface element. Let us apply the theorem to this case. Let us construct a closed surface around the plasmoid, as dotted on Fig. 7. Below, it passes between the central electrode and the plasmoid, so at top it passes above the plasmoid. The integral consists of two parts corresponding to these two parts of the surface with the various direction of the electric field. The first part of the surface is a portion which intersects the plasma jet. The field is directed inward the plasmoid, and the surface area is small. The second part is the entire remaining surface including the streamers and the area above the plasmoid. The field is bigger here and the area of this part of the surface is significantly bigger. Therefore, the integral is defined by the second part. The integral across the whole surface is not zero, and it means that the plasmoid has the electric charge.

This situation refers to the second half of the current phase. The measurements show that the charge exists in the autonomous phase, too. It should be understood that after turning off the discharge current the plasmoid charge does not drain to one or another electrode.

The current flows through the circuit: the high-voltage pole of the condenser—the switch—the central electrode—the plasma jet—the plasmoid—the streamers (at the end of the discharge they look like the skirt)—water—the grounded ring electrode. The switch is designed to operate to introduce a large and highly increasing resistance between the plasmoid center and the high-voltage pole of the condenser (Fig. 1). The discharge current is decreasing. The plasma on the current path cools down. The plasma jet above the central electrode cools down in the fastest way, as it has the small diameter and the high temperature. Here, the conductivity is quickly decreasing. At the same time, the plasma in the skirt cools down more slowly, as its volume is big and the temperature is relatively low. Finally, the resistance between the plasmoid and the high-voltage output of the condenser becomes big. The plasmoid keeps the charge. It can be said that the charge is kept due to fast increase of the resistance on the current path in the sections: the plasma in the switch, the plasma jet, the plasmoid, the plasma in the streamers.

## 7. Comparison of the measured charged with the charge in the plasmoid model

Thus, the plasmoid charge is measured at various time of its existence. The obtained data are extrapolated to the moment of the discharge current break to show that the negative plasmoid has the charge of about  $-35 \text{ nC}$  at this moment. The plasmoid potential at this moment has been evaluated above. The plasmoid radius can be determined from the photos. It has been demonstrated above that the radius of the charge distribution is by 2 cm

larger than the plasmoid radius. Thus, the radius of charge distribution in the plasmoid can also be evaluated. Now, it is possible to compare the independently measured charge of the plasmoid, radius of the charge distribution of the plasmoid and potential of the central electrode by accepting the model, in which the plasmoid and the surrounding grounded equipment are a spherical condenser.

By definition, the spherical condenser consists of two spherical linings and a dielectric therebetween. The parameters of the charged condenser are described by the formula

$$Q = \varphi \varepsilon / (1/R_1 - 1/R_2) / k,$$

where  $Q$  — the condenser charge,  $\varphi$  — the difference of the potentials between the linings,  $\varepsilon$  — the relative permittivity of the dielectric between the plates,  $R_1, R_2$  — the radii of the internal and external spherical lining of the condenser, the constant  $k = 1/4\pi\varepsilon_0$ ,  $\varepsilon_0$  — the electric constant. Numerically,  $k = 9 \cdot 10^9 \text{ V}\cdot\text{m}/\text{C}$ .

In this case, the internal lining is a plasmoid with the radius (more exactly, the radius of charge distribution)  $R_1$ .

In the particular case, the radius of the external lining can be either significantly higher than the radius of the internal lining or infinite. Then, the magnitude  $1/R_2$  can be neglected. In this case, the external lining is not spherical and consists of such items as the ring electrode, the grounded wires of the power and measurement system, the grounded wires of the laboratory, the frame. The distance to them is 0.5–2 m, i.e.  $R_2$  is in 5–20 times bigger than  $R_1$ . Let us neglect the magnitude  $1/R_2$ , which turns out to be smaller in comparison with  $1/R_1$ . Then, the parameters of the charged condenser are formulated as  $Q = \varphi \varepsilon R_1 / k$ .

When the discharge current flows, the condenser is charged, as the internal lining of the condenser (i.e., the plasmoid) is connected by a conductor (plasma jet) to the high-voltage central electrode. This connection disappears in the autonomous phase, and the spherical plasmoid becomes electrically isolated.

The charge and the potential have been evaluated above. Judging by the records, at the moment of the current break the glow radius of the plasmoid was 7.5 cm. The analysis of the Section 5 has shown that at the time of 300 ms and more the distribution of the charge in the plasmoid is more than the glow distribution approximately by 2 cm. Taking this into account, the radius of the charge distribution is

$$R_1 = 7.5 \text{ cm (glow radius)} + 2 \text{ cm} = 9.5 \text{ cm}.$$

Inserting the values of  $\varphi$  and  $R_1$  into the condenser formula  $Q = \varphi \varepsilon R_1 / k$ , we obtain that the so-evaluated charge is  $-24.3 \text{ nC}$ . This value should be compared with the charge  $-35 \text{ nC}$  extrapolated in accordance with the experimental data (Fig. 3). Taking into account uncertainties, assumptions and that we are taking about a new phenomenon, the agreement is quit good.

In the plasmoid model as the spherical condenser, the plasmoid charge is proportional to its radius at the equal

potentials. As said above, the sizes of the negative plasmoids are bigger than sized of the positive plasmoids. Probably, it is one of the reasons why the charges of the negative plasmoids have turned out to be higher than the positive ones.

Based on the obtained data on the charge, let us evaluate the electric field on the plasmoid surface at the end of the discharge current, i.e. 130 ms. The radius of the charge distribution  $R_1$  has been evaluated above. In accordance with these experimental data, we obtain that the field  $E = Q \cdot k / (R_1)^2 = 35 \cdot 10^{-9} \cdot 9 \cdot 10^9 / (0.095)^2 \cong 35 \text{ kV}/\text{m}$ . This value should be compared with the breakdown field at the normal conditions, which is 3000–3300 kV/m. As you can see, the field on the plasmoid surface is in 86–94 times less than the breakdown one. This result agrees with the fact that no spark or other discharge is observed around the plasmoid.

## 8. Discussion and conclusion

The work has continued to investigate the long-lived plasmoid originating in the atmosphere at the high-voltage discharge above the water surface. The previously-detected electric charge of the plasmoid has been investigated in more detail. The charge has been measured using the modified Langmuir probe. The probe is manufactured as a wire grid installed at a path of the rising plasmoid. The grid collects the charged particles due to their drift motion in the electric field created by the plasmoid charge, and due to the diffusion movement of the particles. The data on the charge are provided by the drift current. If the drift current is much bigger than the diffusion one, then the plasmoid charge is equal to the current integral for the time of the plasmoid passing through the grid. It has been found during the investigation that there was also the bias current. It is created by the electric field of the plasmoid and the field of the laboratory instruments. The bias current was taken into account by using an additional grid designed to measure the bias current. This grid is made of the insulated wire. The grounded (reference) electrode for the grids is presented by the ring electrode in water.

As expected, the sign of the measured charge of the plasmoid coincides with the sign of the potential of the central electrode of the grounded ring electrode. Although the charge is a remaining magnitude, it turned out that the higher the grid above water, the smaller the measured charge is. It is caused by the reduction of the mobility and the concentration of the charged particles in time, thereby resulting in the decrease of the drift current.

Using the obtained data, by extrapolation, the charge  $Q$  of the negative plasmoid was evaluated at the moment of turning off the discharge current. The charge is about  $-35 \text{ nC}$ . This extrapolated charge, radius of charge distribution in the plasmoid  $R_1$  and potential of the central electrode  $\varphi$  (all the values refer to the moment of the discharge current break) are independently measured magnitudes. It

has turned out that these value approximately meet the formula  $Q = \varphi \cdot R_1/k$ , which describes the parameters of the charged sphere, which is a particular case of the spherical condenser, whose radius of the external lining is significantly bigger than the radius of the internal one.

The investigation has been carried out so as to say about a mechanism of formation of the plasmoid charge. Let us show that the charge is formed when the discharge current flows. In order to clarify the mechanism, let us apply the Gauss theorem.

The discharge current goes from the central electrode into the plasmoid through the bright plasma jet. From the plasmoid, the current flows through the streamers to water. The current density on the path is different. The jet has a small diameter. The current in it goes through an emission plasma (the lines of electrode metal ions were observed). The current density is big, the temperature of the plasma and its conductivity are high. The electric field is small and directed inward the plasmoid (for the positive plasmoid). From the plasmoid to water the current flows through the streamers, which have the large cross-section. The current density in the streamers is small, the conductivity of the plasma is small in comparison with these parameters in the jet. The electric field is directed outward the plasmoid and it is bigger than the field in the jet. Above the plasmoid, the field is also directed outward, which is manifested by the measurements of the potential. Knowing the distribution of the electric field, it is possible to evaluate the integral from the normal component of the field over a certain closed surface surrounding the plasmoid. For the evaluation, it is important that the section of the current and the field value in the streamers is significantly higher than these parameters in the plasma jet. Hence, the integral is determined by a surface part, in which the field is directed outward the plasmoid. It is a surface on the side of the plasmoid (which intersects the streamers) and on top of the plasmoid. It is obvious, that the integral is not zero. In other words, the plasmoid carries the electric charge.

After turning on the discharge current, the plasma in the plasma jet above the central electrode quickly cools down, as its volume is small and its temperature is high. The conductivity between the plasmoid and the electrode disappears. Therefore, the plasmoid charge does not drain to the central electrode.

The investigation has been carried out, so the experiment conditions can be selected to affect the electric charge of the plasmoid. Probably, with increase of the discharge voltage it is possible to obtain the plasmoid with the big charge, of course, provided that the relationship disclosed in the present work is satisfied: the electric resistance of the plasma jet is significantly smaller than the resistance of the streamers.

This investigation additionally supports the hypothesis that the electric charge is a common property of the ball lightning and the plasmoid. The present investigation also raises the question of relation between the electrical and gas dynamic properties of the plasmoid. This complicated

question could not be considered within the performed investigation.

In conclusion. In our view, the plasmoid is a charged cloud of erosion plasma, which exists in the atmosphere for a long time.

## Acknowledgments

The author would like to thank the A. V. Arutyunyan and G. D. Shabanov for permanent discussion of the work, S. R. Gurin and A. P. Roganov for help in manufacturing the equipment and A. A. Vaganov for his initiative in carrying out additional experiments and participation therein.

## Conflict of interest

The author declares that he has no conflict of interest.

## References

- [1] J.D. Barry. *Ball Lightning and Bead Lightning* (Plenum, NY, 1980)
- [2] V.N. Kunin. *Sharovaya molniya na eksperimental'nom poligone* (Gos. universitet, Vladimir, 2000) (in Russian).
- [3] L.V. Furov. *Tech. Phys.*, **50** (3), 380 (2005). DOI: 10.1134/1.1884742
- [4] G.S. Paiva, A.C. Pavao, E. Alpes de Vasconcelos, O. Mendes, Jr., E. Felisberto da Silva Jr. *Phys. Rev. Lett.*, **98**, 048501 (2007). DOI: 10.1103/PhysRevLett.98.048501
- [5] G.D. Shabanov, A.G. Krivshich, B.Yu. Sokolovskiy, O.M. Zhrebtsov. *Trudy mezhd. konf. Estestvennye i antropogennye aerezoli* (SPb., 2001), v. 3, p. 368 (in Russian).
- [6] G.D. Shabanov. *Tech. Phys. Lett.*, **8** (2), 164 (2002). DOI: 10.1134/1.1458524
- [7] A.I. Egorov, S.I. Stepanov. *Tech. Phys.*, **47** (12), 1584 (2002). DOI: 10.1134/1.1529952
- [8] A.I. Egorov, S.I. Stepanov, G.D. Shabanov, *Phys. Usp.*, **47** (1), 99 (2004). DOI: <http://dx.doi.org/10.1070/PU2004v047n01ABEH001691>
- [9] R. Friedl, U. Fantz, I. Pilottek, D. Schmid, S. Steibel. *J. Phys. D: Appl. Phys.*, **54**, 095205 (2021). DOI: 10.1088/1361-6463/abc918
- [10] V.L. Bychkov, S.V. Anpilov, N.P. Savenkova, V. Stelmashuk, P. Hoffer. *J. Physics: Conf. Series*, **996**, 012012 (2018). DOI: 10.1088/1742-6596/996/1/012012
- [11] V.L. Bychkov. *Estestvennye i iskustvennye sharovye molnii v atmosfere Zemli* (Maks Press, M., 2021) (in Russian) DOI: 10.29003/m2009.978-5-317-06572-0
- [12] J.R. Powell, D. Finkelstein. *Adv. Geophys.*, **13**, 141 (1969).
- [13] M.L. Shmatov, K.D. Stephan. *J. Atmos. Sol.-Ter. Phys.*, **195**, 105115 (2019).
- [14] I.P. Stakhanov. *O fizicheskoy prirode sharovoy molnii* (Energoatomizdat, M, 1985) (in Russian).
- [15] A.I. Grigor'ev, S.O. Shiryaeva, N.A. Petrushov. *Tech. Phys.*, **61** (9), 1319 (2016). DOI: 10.1134/S1063784216090085
- [16] M.T. Dmitriev. *ZhTF*, **39** (2), 387 (1969) (in Russian).
- [17] M.L. Shmatov. *J. Plasma Phys.*, **69** (6), 507 (2003). DOI: 10.1017/S002237780300237X
- [18] A.I. Egorov, S.I. Stepanov. *Tech. Phys.*, **53** (6), 688 (2008). DOI: 10.1134/s1063784208060029

- [19] A. Versteegh, K. Behringer, U. Fantz, G. Fussmann, D. Jutter, S. Noack. *Plasma Sources Sci. Technol.*, **17**, 024014 (2008). DOI: 10.1088/0963-0252/17/2/024014
- [20] S.I. Stepanov, *Tech. Phys.*, **59**(1), 107 (2014). DOI: 10.1134/S1063784214010198
- [21] G.A. Kukekov. *Proektirovanie vyklyuchateley peremennogo toka vysokogo napryzheniya* (Gosenergoizdat, M.–L., 1961) (in Russian).
- [22] Y. Sakawa, K. Sugiyama, T. Tanabe, R. More. *Plasma and Fusion Research.*, **1**, 039 (2006). DOI: 10.1585/pfr.1.039
- [23] B. Juettner, S. Noack, A. Versteegh, G. Fussmann. *Long-Living Plasmoids from a Water Discharge at Atmospheric Pressure. Proc. 28th ICPIG* (Prague, Czech Republic, 2007), July 15–20, p. 2229–34
- [24] A. Versteegh. *Master Thesis* (Technische Universiteit, Eindhoven, 2007)
- [25] S. Noack. *Diploma Thesis* (Universitat Leipzig, Leipzig, 2008)
- [26] K.D. Stephan, Sh. Dumas, L. Komala-Noor, J. McMinn. *Plasma Sources Sci. Technol.*, **22**, 025018 (2013). DOI: 10.1088/0963-0252/22/2/025018
- [27] D.M. Friday, P.B. Broughton, T.A. Lee, G.A. Schutz, J.N. Betz, C.M. Lindsay. *J. Phys. Chem. A*, **117**(39), 9931 (2013). DOI: 10.1021/jp400001y
- [28] U. Fantz, S. Kalafat, R. Friedl, S. Briefi. *J. Appl. Phys.*, **114**, 043302 (2013). DOI: 10.1063/1.4816311
- [29] D.M. Friday. *Master Thesis* (University of Illinois, Urbana, 2014)
- [30] U. Fantz, S. Briefi, R. Friedl, M. Kammerloher, J. Kolbinger, A. Oswald. *IEEE Transactions on Plasma Science*, **42**(10), (2014). DOI: 10.1109/tps.2014.2310128
- [31] S.C. Dubowsky. *Doctor Dissertation* (University of Illinois, Urbana, 2018)
- [32] S. Zhao, C. Yuan, A.A. Kudryavtsev, O.M. Zherebtsov, G.D. Shabanov. *Tech. Phys.*, **66**(9), 1058 (2021). DOI: 10.1134/S1063784221070173
- [33] S.E. Dubowsky, D.M. Friday, K.C. Peters, Z. Zhao, R.H. Perry, B.J. McCall. *Intern. J. Mass Spectrometry*, **376**, 39 (2015). DOI: <http://dx.doi.org/10.1016/j.ijms.2014.11.011>
- [34] C.J.V. Wurden, G.A. Wurden, *IEEE Transactions on Plasma Science*, **39**(11), 2078 (2011). DOI: 10.1109/TPS.2011.2155090
- [35] S.E. Dubowsky, A.N. Rose, N.G. Glumac, B.J. McCall. *Plasma*, **3**(3), 92 (2020). DOI: 10.3390/plasma3030008
- [36] S.E. Dubowsky, B. Deutsch, R. Bhargava, B.J. McCall. *J. Molecular Spectroscopy*, **322**, 1 (2016). DOI: <http://dx.doi.org/10.1016/j.jms.2016.02.005>
- [37] M. Jacobs, W. Gekelman, P. Pribyl, Y. Qian, S. Abarzhi. *Phys. Plasmas*, **28**, 052114 (2021). DOI: 10.1063/5.0040880
- [38] U. Fantz, S. Briefi, R. Friedl, M. Kammerloher, A. Oswald, D. Rauner. 30th ICPIG, August 28th — September 2nd 2011, Belfast, Northern Ireland, UK.
- [39] V. Stelmashuk, P. Hoffer. *IEEE Transaction on Plasma Science*, **45**(12), 3160 (2017). DOI: 10.1109/TPS.2017.2770224